УДК 621.317

*DOI*: https://doi.org/10.20535/0203-3771432022275285

**A. Prach**[1], *Assistant Professor*

# SDC-BASED DYNAMIC INVERSION CONTROLLER FOR A FIXED-WING AIRCRAFT

**Ua** В даній роботі представлено систему керування, що використовує інверсію динамічної моделі та матриці коефіцієнти яких залежать від стану. Система керування застосований для проблеми орієнтації та керування швидкістю літака. Чисельна перевірка запропонованого регулятора виконана з використанням симуляційної моделі літака *Cessna* 172 для кількох сценаріїв атмосферних збурень.

**En** This work presents dynamic model inversion controller which uses state dependent coefficient matrices, and is applied for a fixed-wing aircraft attitude and velocity control problem. Numerical validation of the proposed controller is done using a Cessna 172 aircraft simulation model for several scenarios of atmospheric disturbances.

## Introduction

The objective of this paper is to present a method for the design of a nonlinear flight controller for a fixed-wing aircraft using a state-dependent-coefficient (SDC) based model inversion approach. This approach involves a parameterization of the aircraft nonlinear dynamics into a linear-like structure that is later used in the model inversion algorithm.

Dynamic inversion control is often utilized for the flight control systems thanks to the simplicity of the concept [1]. [2] discusses the use of nonlinear dynamic inversion for a flight control system design for a supermaneuverable

[1] *Middle East Technical University, Northern Cyprus Campus*

aircraft. In the proposed approach, separate approximate dynamic inversion control laws are designed for fast and slow dynamic variables. In [3] dynamic inversion is achieved via feedback linearization, and applied for longitudinal control of an aircraft. [4] also uses feedback linearization for a hypersonic vehicle control. Dynamic inversion is often used in a combination with other control methods [5–7].

In linear control techniques, dynamic inversion uses linearized dynamics yielding a simple controller structure. A disadvantage of this approach is that a linear model is valid within a certain neighbourhood around the linearization point, and may not capture dynamic coupling and nonlinearities in aircraft dynamics. Nonlinear model inversion results to a more complex control structure. Another problem associated with the model inversion is the control allocation.

In this paper, a nonlinear model inversion uses a nonlinear model, which is represented by a linear structures based on the state-dependent coefficient (SDC) parameterization. SDC parameterization (often called SDC factorization) is originally proposed in state-dependent Riccati equation (SDRE) control [8 - 11] and estimation [12 - 14]. It involves representing nonlinear dynamics $\dot{x} = f(x,u)$ in the form $\dot{x} = A(x)x + B(x)u$, where $A(x)$ and $B(x)$ are state-dependent coefficient matrices. SDC factorization represents the actual nonlinear dynamics, and allows capturing coupling in the system dynamics. Moreover, SDC model is valid throughout the entire operating envelope due to the fact that the state-dependent-coefficient matrices $A(x)$ and $B(x)$ are updated continuously using the state measurements or estimations. It should be noted that SDC parameterization is not unique, and thus the choice of SDC may impact stability and performance. The SDC-parameterized model can be used for dynamic inversion control yielding a nonlinear SDC-based dynamic inversion.

In this paper, a nonlinear SDC-based dynamic inversion is used in the inner-loop of the attitude controller, the goal of which is to provide attitude command following and stabilization in the presence of atmospheric disturbances such as wind gust and turbulence. SDC model inversion is based on the aircraft rotational dynamics, and yields the actuator deflections required to achieve the desired command following. The velocity-hold controller is represented by a classical nonlinear model inversion, and provides a required throttle input to maintain the desired velocity. Command filters are used to shape the desired commands to avoid the saturations of the control actuators. The effectiveness of the introduced control architecture is validated by numerical simulations using a Cessna 172 aircraft model. Numerical studies are carried out for different crosswind and turbulence conditions.

The paper is organized as follows. Section 1 provides a brief discussion of the model inversion method and presents the methodology of the SDC-based

model inversion. Section 2 covers the controller structure including the attitude and velocity- hold controllers. The next section described the simulation model, including the atmospheric models, and is followed by numerical simulation results. Conclusions are provided in the final section.

**SDC Dynamic Inversion**

The idea behind dynamic inversion for linear systems is rather simple. Consider an LTI system written in the standard state- space form,

$$\dot{\mathbf{x}}(t) = A\mathbf{x}(t) + B\mathbf{u}(t) \tag{1}$$

where $\mathbf{x}(t) \in \mathbb{R}^n$, $\mathbf{u}(t) \in \mathbb{R}^m$. The control law $\mathbf{u}(t)$ that generates the desired dynamic response $\dot{\mathbf{x}}_{\text{des}}(t)$ is obtained as follows

$$\mathbf{u}(t) = B^{-1}[\dot{\mathbf{x}}_{\text{des}}(t) - A\mathbf{x}(t)] \tag{2}$$

where the state vector $\mathbf{x}(t)$ is assumed to be measured, and matrices $A$ and $B$ are known. Note that (2) requires the input matrix $B$ to be invertible. This requirement implies that for when the number of control inputs (independent control effectors) is equal to the number of states, model inversion is straight forward. However, if the number of control inputs is greater than the number of the effects that they generate, a control allocation must be implemented [1].

Consider a nonlinear system given by the state equations in the form

$$\dot{\mathbf{x}}(t) = \mathbf{f}(\mathbf{x}(t), \mathbf{u}(t)) \tag{3}$$

where for all $\mathbf{x}(t) \in \mathbb{R}^n$, $\mathbf{u}(t) \in \mathbb{R}^m$, $\mathbf{f}(\mathbf{x}(t), \mathbf{u}(t)) \in \mathbb{R}^n$. Assume that (3) can be written in the SDC form [10]

$$\dot{\mathbf{x}}(t) = A(\mathbf{x}(t))\mathbf{x}(t) + B(\mathbf{x}(t))\mathbf{u}(t) \tag{4}$$

where $A(\mathbf{x}(t)) \in \mathbb{R}^{n\times n}$ and $B(\mathbf{x}(t)) \in \mathbb{R}^{n\times m}$. A parameterization (4) exists under the assumptions $\mathbf{f} \in \mathbb{C}^1$ and $\mathbf{f}(0) = 0$. In addition, if $n > 2$, then $A(\mathbf{x}(t))$ is not unique.

From (4), the control law $\mathbf{u}(t)$ that generates the desired dynamic response $\dot{\mathbf{x}}_{\text{des}}(t)$ is obtained as follows

$$\mathbf{u}(t) = B(\mathbf{x}(t))^{-1}[\dot{\mathbf{x}}_{\text{des}}(t) - A(\mathbf{x}(t))\mathbf{x}(t) \tag{5}$$

where $B(\mathbf{x}(t))$ must be invertible for all $\mathbf{x}(t)$.

**Controller Structure**

The block diagram of the controller structure is given in Fig. 1. The first channel is a dual-loop altitude controller, which includes the SDC dynamic inversion. The second control channel is the velocity-hold controller. The desired attitude commands can be defined directly, or obtained from the additional position controller. The attitude commands $[\phi_{\text{des}}\ \theta_{\text{des}}\ \psi_{\text{des}}]^T$ are

shaped using the second order command filters that smooth out the commands yielding $[\phi_c \ \theta_c \ \psi_c]^T$. Addition of the command filters reduces the chances of actuator saturation, and provides the attitude commands that are feasible for the aircraft to follow.

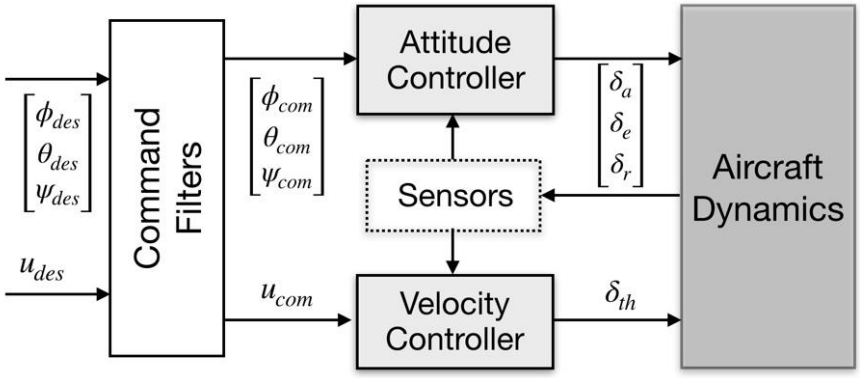


Fig. 1. Controller block diagram

Fig. 2 shows the block diagram of the attitude controller. For the given attitude reference commands, the outer-loop controller generates the desired angular accelerations that are transformed into the body axis $[p_{\text{des}} \ q_{\text{des}} \ r_{\text{des}}]^T$, and form an input for the SDC dynamic inversion. The outer-loop controller uses a conventional PID control algorithm. The SDC dynamic inversion uses the measurements of the aircraft angular rates.

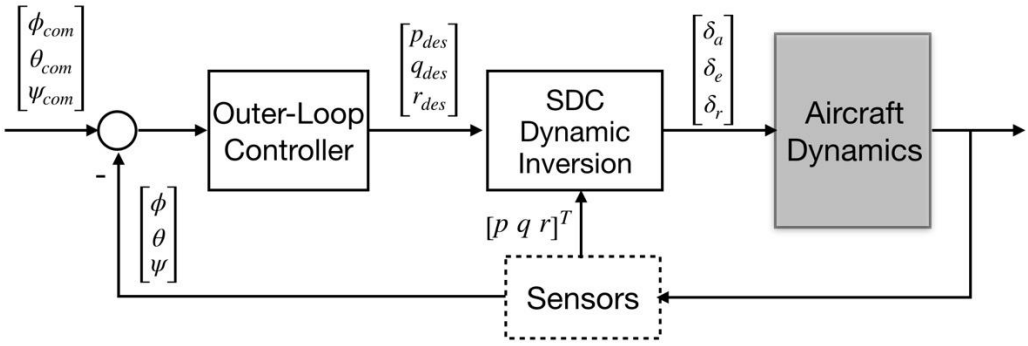


Fig. 2. Attitude controller block diagram

**SDC Dynamic Inversion for Aircraft Rotational Dynamics**

The SDC dynamic inversion controller is obtained from the rotational dynamics of a fixed-wing aircraft [15], and forms the inner-loop of the attitude controller.

Consider the angular dynamics of the aircraft, given by

$$I_{xx}\dot{p} - I_{xz}\dot{r} + I_{xz}pq + \left(I_{zz} - I_{yy}\right)qr = L, \tag{6}$$

$$I_{yy}\dot{q}+\left(I_{xx}-I_{zz}\right)pr+I_{xz}\left(p^2-r^2\right)=M, \tag{7}$$

$$I_{zz}\dot{r}-I_{xz}\dot{p}+I_{xz}qr+\left(I_{yy}-I_{xx}\right)pq=N, \tag{8}$$

where $p, q, r$ represent the components of the angular velocity vector defined in the body axis, $L, M, N$ are the rolling, pitching, and yawing moments, respectively. $I_{xx}, I_{yy}, I_{zz}, I_{xz}$ are the components of the inertia tensor. The aerodynamic moments are the functions of aerodynamic stability and control derivatives [15]

$$L=L_{\beta}\beta+L_p p+L_r r+L_{\delta_a}\delta_a+\ L_{\delta_r}\delta_r, \tag{9}$$

$$M=M_u\,\Delta u+\frac{M_{\alpha}}{u_{tr}}\Delta w+M_q q+M_{\delta_e}\delta_e, \tag{10}$$

$$N=N_{\beta}\beta+N_p p+N_r r+N_{\delta_a}\delta_a+\ N_{\delta_r}\delta_r, \tag{11}$$

where $\Delta u=u-u_{tr}$, $\Delta w=w-w_{tr}$. $u_{tr}$ and $w_{tr}$ are the trim values of the components of the linear velocity vector in the *x* and *z*-body axis. The aerodynamic stability and control derivatives are defined using the aerodynamic coefficients [15]. In the vector and matrix form, (6) – (8) can be written as

$$A_1\begin{bmatrix}\dot{p}\\ \dot{q}\\ \dot{r}\end{bmatrix}-A_2\begin{bmatrix}p\\ q\\ r\end{bmatrix}+A_3\begin{bmatrix}\beta\\ \Delta u\\ \Delta w\end{bmatrix}=B\begin{bmatrix}\delta_a\\ \delta_e\\ \delta_r\end{bmatrix}, \tag{12}$$

where

$$A_1=\begin{bmatrix}I_{xx} & 0 & -I_{xz}\\ 0 & I_{yy} & 0\\ -I_{xz} & 0 & I_{zz}\end{bmatrix},$$

$$A_2=\begin{bmatrix}L_p-I_{xz}q & 0 & L_r-\left(I_{zz}-I_{yy}\right)q\\ \left(I_{xx}-I_{zz}\right)r+I_{xz}p & M_q & I_{xz}r\\ N_r-\left(I_{yy}-I_{xx}\right)q & 0 & N_p-I_{xz}q\end{bmatrix}, \tag{13}$$

$$A_3 = \begin{bmatrix} L_\beta & 0 & 0 \\ 0 & M_u & M_\alpha / u_{tr} \\ N_\beta & 0 & 0 \end{bmatrix}, \quad B = \begin{bmatrix} L_{\delta_a} & 0 & L_{\delta_r} \\ 0 & M_{\delta_e} & 0 \\ N_{\delta_a} & 0 & N_{\delta_r} \end{bmatrix},$$

where the SDC matrix $A_2$ depends on the components of the angular velocity vector $\begin{bmatrix} p & q & r \end{bmatrix}^T$, and is continuously updated with the angular velocity measurements. It should be noted that the choice of the matrix $A_2$ is not unique, but the other matrices are fixed.

The desired angular accelerations, which are obtained from the outer-loop attitude controller, are defined as $\dot{p} = \dot{p}_{\text{des}}$, $\dot{q} = \dot{q}_{\text{des}}$, $\dot{r} = \dot{r}_{\text{des}}$ . Under assumption that matrix $B$ is invertible, the required actuator deflections $\delta_a$, $\delta_e$, $\delta_r$ can be found as follows

$$\begin{bmatrix} \delta_a \\ \delta_e \\ \delta_r \end{bmatrix} = B^{-1} \left( A_1 \begin{bmatrix} \dot{p}_{\text{des}} \\ \dot{q}_{\text{des}} \\ \dot{r}_{\text{des}} \end{bmatrix} - A_2 \begin{bmatrix} p \\ q \\ r \end{bmatrix} + A_3 \begin{bmatrix} \beta \\ \Delta u \\ \Delta w \end{bmatrix} \right). \tag{14}$$

Note that matrix $B$ includes the control derivatives $L_{\delta_a}$, $L_{\delta_r}$, $M_{\delta_e}$, $N_{\delta_a}$, $N_{\delta_r}$, which represent the effect of the control surfaces on the corresponding angular moments. For a fixed-wing aircraft this matrix is invertible.

**Velocity Controller**

The velocity controller consists of a PI controller combined with a nonlinear model inversion, and generates the throttle input to achieve a desired velocity. A first order command filter is added to shape the desired velocity command $u_{\text{com}}$ taking into account the engine dynamics.

The desired linear acceleration in $x$-body axis, $\dot{u}_{\text{des}}$ is generated as an output of the PI controller with the gains $K_{p_u}$, $K_{i_u}$ as follows

$$\dot{u}_{\text{des}} = K_{p_u} \left( u_{\text{com}} - u \right) + K_{i_u} \int \left( u_{\text{com}} - u \right). \tag{15}$$

The throttle input is obtained from the nonlinear inversion of the translational longitudinal dynamics

$$m\left( \dot{u} + qw - rv \right) = X - mg \sin\theta \tag{16}$$

where the aerodynamic force $X$ given in terms of dimensional stability and control derivatives as follows

$$X = \left( X_u + X_{\delta_T} \right) \Delta u + \frac{X_\alpha}{u_{tr}} \Delta w + X_{\delta_{th}} \delta_{th}. \tag{17}$$

The aerodynamic stability and control derivatives are defined using the aerodynamic coefficients [15]. Let $\dot{u} = \dot{u}_{\text{des}}$, and combining (16), (17) yields the required throttle input $\delta_{th}$

$$\delta_{th} = \frac{1}{X_{\delta_{th}}}\left[ m\left(\dot{u}_{\text{des}} + qw - rv\right) - \left(X_u + X_{\delta_T}\right)\Delta u + \frac{X_\alpha}{u_{tr}}\Delta w - mg\sin\theta \right] \tag{18}$$

**Numerical Simulations**

Numerical simulations are carried out to test and validate the performance of the proposed control algorithms for the Cessna 172 aircraft. A high fidelity simulation model of the aircraft is developed using the 6 DOF equations of motion. The aircraft is equipped with the traditional aerodynamic control surfaces that is elevator for pitch control, rudder for yaw control, and ailerons for roll control. The simulation model includes realistic models for the engine actuator and sensor dynamics. The propulsion system is modelled using the propeller and engine parameters, and the aircraft's speed. The simulation model also includes the actuator deflection and the deflection rate limits. The atmospheric conditions are represented by the standard atmosphere model (COESA). The wind gust and wind turbulence models are based on the Military Specification MIL-F-8785C. The following subsections show the numerical simulation results for the stabilization problems with different atmospheric conditions including still atmosphere, turbulence, turbulence with headwind and sidewind. The goal of the controller is first to trim the airplane starting from the specific initial conditions, and provide stabilization in case of the presence of any atmospheric disturbances. The aircraft is commanded to fly straight North (zero yaw), wings level (zero roll) maintaining the velocity of 160 ft/s, and the desired altitude of 8000 ft. Hence, the desired trim values for the roll and yaw angles are zero. The pitch angle command is generated by the altitude controller, which aims to minimize the altitude error.

**Simulation 1: Still Atmosphere**

In the first numerical study the controller trims the airplane in a level flight without atmospheric disturbances. The initial conditions for both the roll and the pitch angles are equal to 5 deg, the initial conditions for the yaw angle is zero. Fig. 3 and Fig. 4 shows the responses of the Euler angles, velocity, altitude error, and horizontal position, respectively. The angle of attack and sideslip angle responses are given in Fig. 5 and show that the angle of attack converges

to a constant trim value, and the sideslip is zero. The actuators demand and propeller RPM are given in Fig. 6.

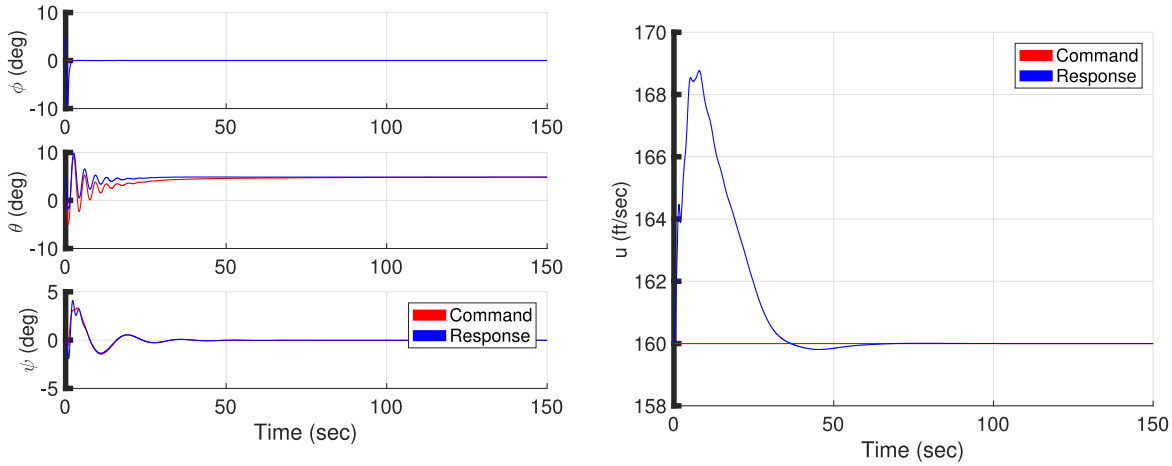


*a*) Euler angles *b*) Velocity

Fig. 3. Simulation 1: Euler angles and velocity responses

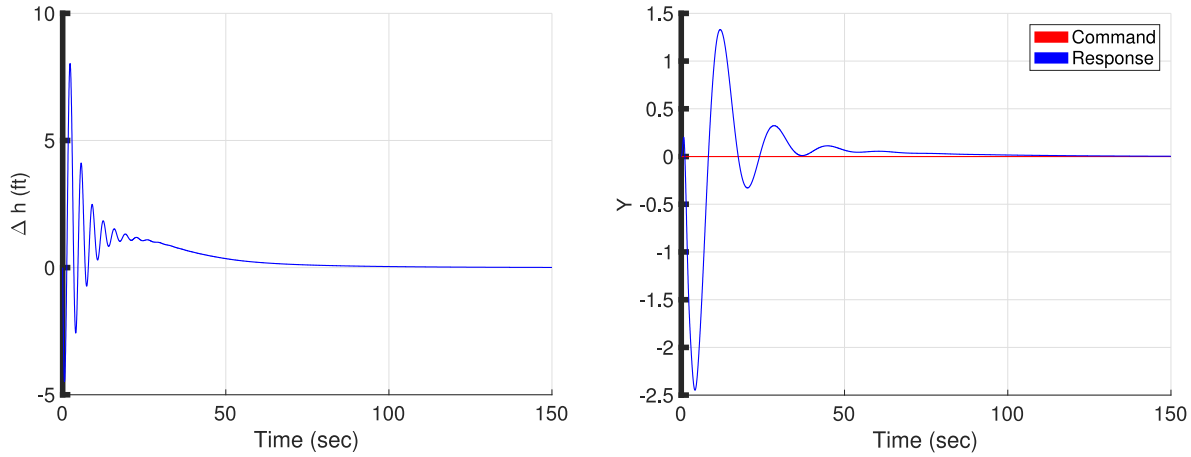


*a*) Altitude error *b*) Horizontal position

Fig. 4. Simulation 1: Altitude error, and horizontal position responses

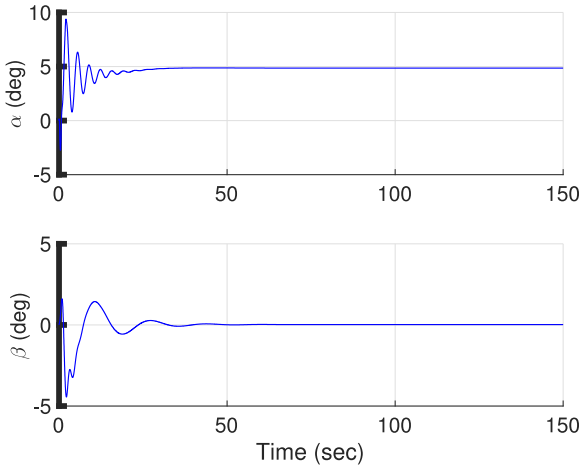


Fig. 5. Simulation 1: Angle of attack and sideslip angle

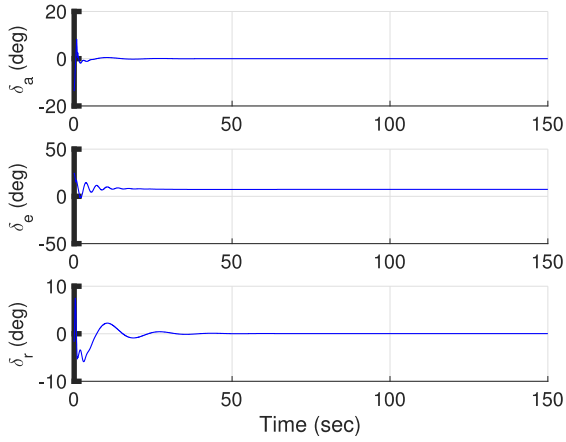


*a*) Aileron, elevator, and rudder positions

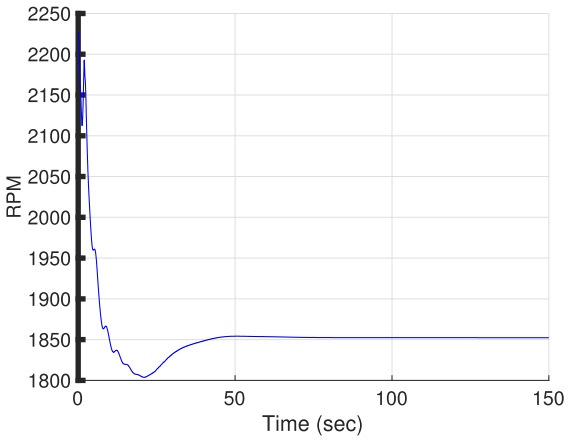


*b*) Propeller RPM

Fig. 6. Simulation 1: Altitude error, and horizontal position responses

**Simulation 2: Light Turbulence**

In the second simulation case, the airplane is stabilized when flying in a turbulent atmosphere with the same initial conditions as in the first simulation case. The wind velocity profile is shown in the Fig. 7. Fig. 8 and Fig. 9 shows the responses of the Euler angles, velocity, altitude error, and horizontal position respectively. The angle of attack and sideslip angle responses are given in Fig. 10. The actuators demand and propeller RPM are given in Fig. 11.

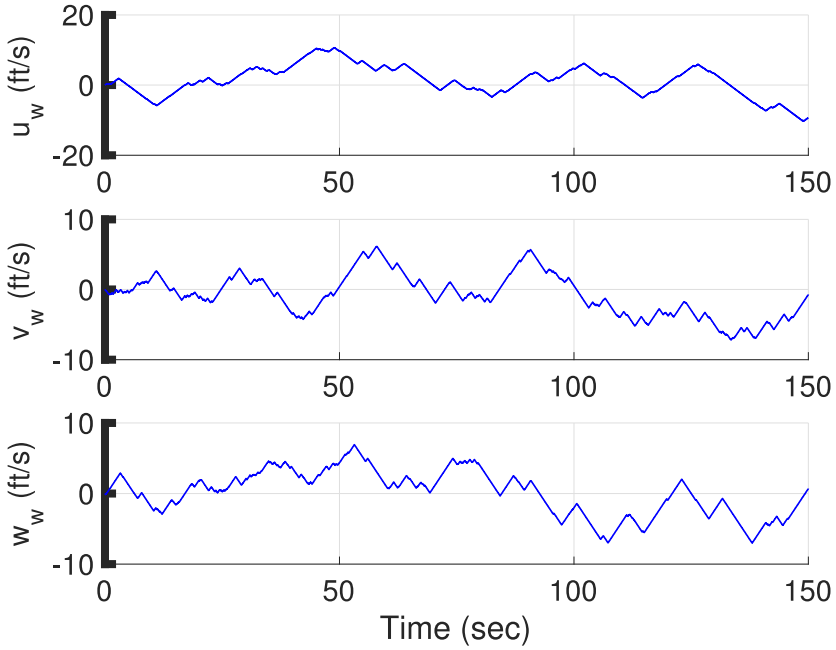


Fig. 7. Simulation 2: Wind velocity profile

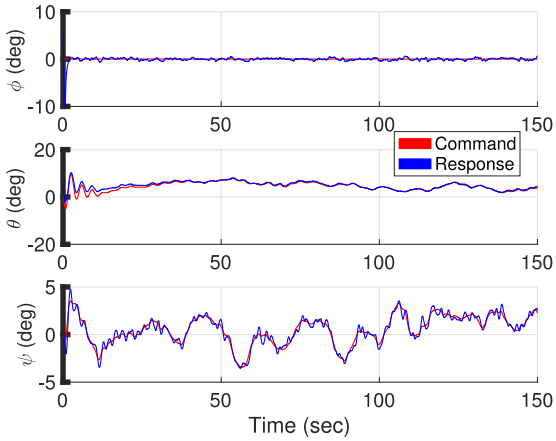


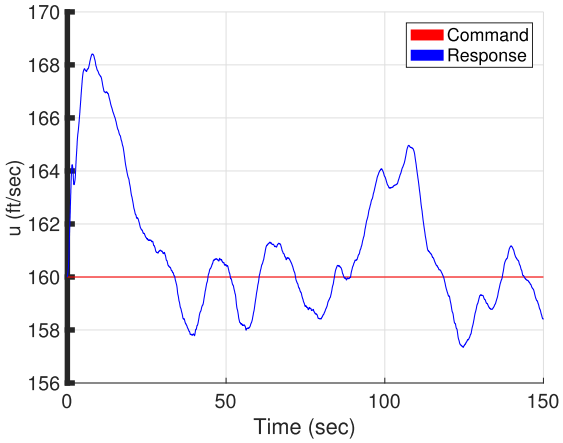


*a*) Euler angles *b*) Velocity

Fig. 8. Simulation 2: Euler angles and velocity responses

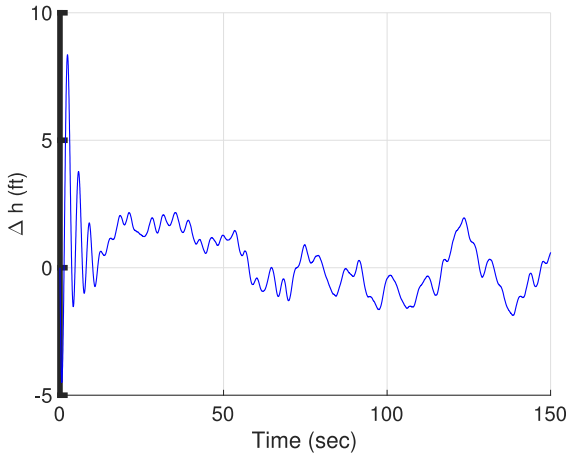


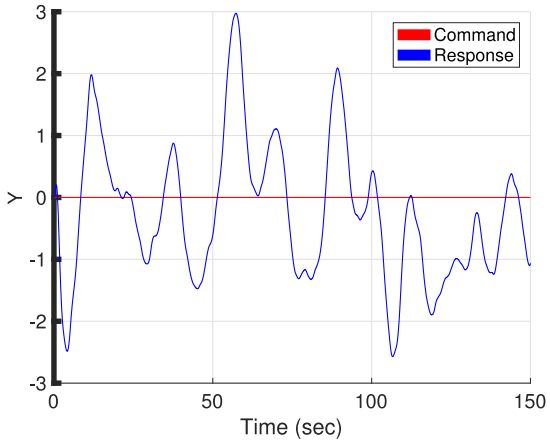


*a*) Altitude error *b*) Horizontal position

Fig. 9. Simulation 2: Altitude error, and horizontal position responses

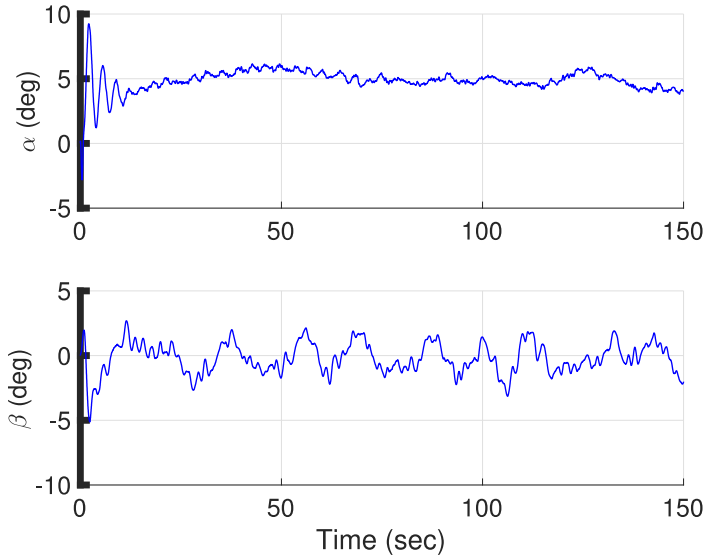


Fig. 10. Simulation 2: Angle of attack and sideslip angle

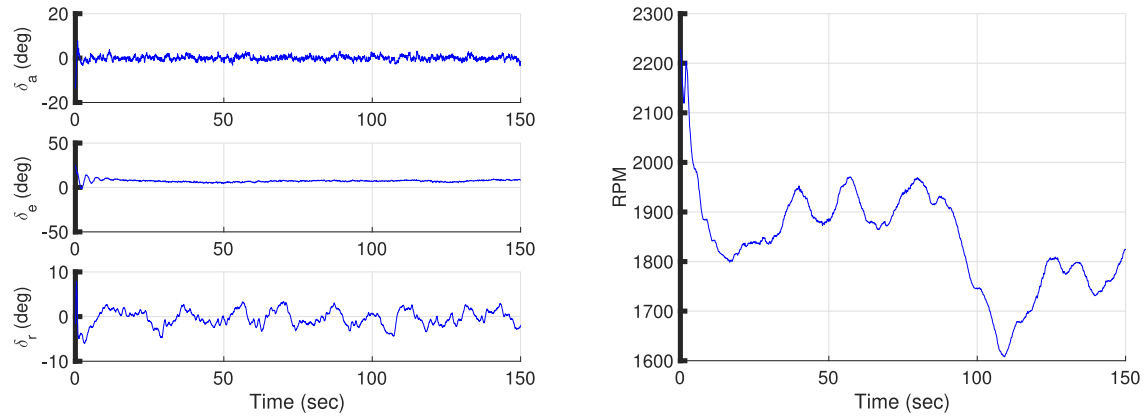


*a*) Aileron, elevator, and rudder positions

*b*) Propeller RPM

Fig. 11. Simulation 2: Altitude error, and horizontal position responses

**Simulation 3: Light Turbulence + Head Wind + Side Wind**

In the last simulation case, the airplane is stabilized while flying in a turbulent atmosphere with the head wind gust and side wind gust of 30 ft/s starting at the 60's second of the simulation. The wind velocity profile is shown in the Fig. 12. Fig. 13, Fig. 14, and Fig. 15 show the corresponding responses. The actuators demand and propeller RPM are given in Fig. 16.

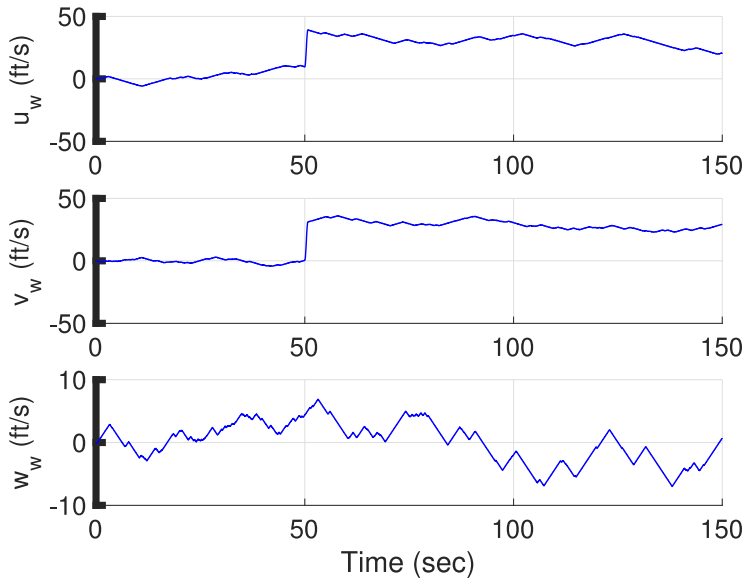


Fig. 12. Simulation 3: Wind velocity profile

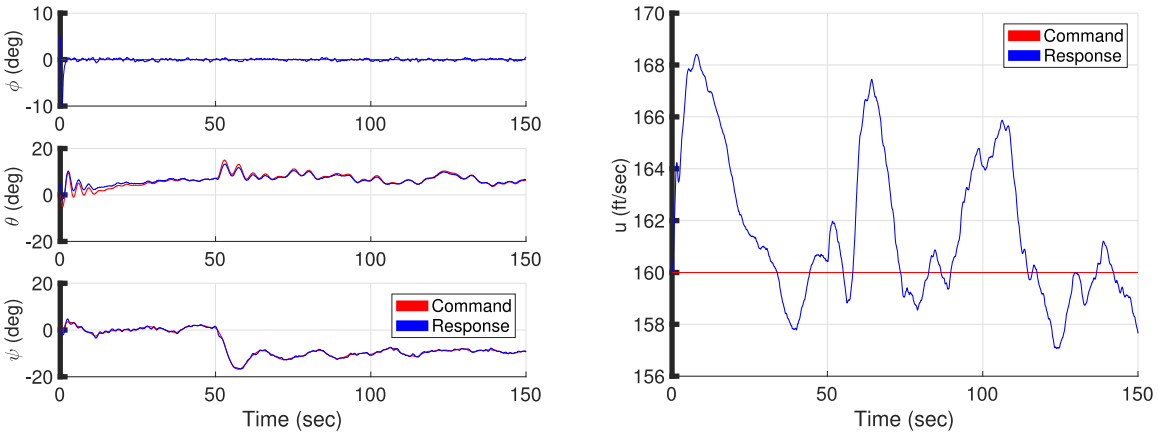


*a*) Euler angles *b*) Velocity

Fig. 13. Simulation 3: Euler angles and velocity responses

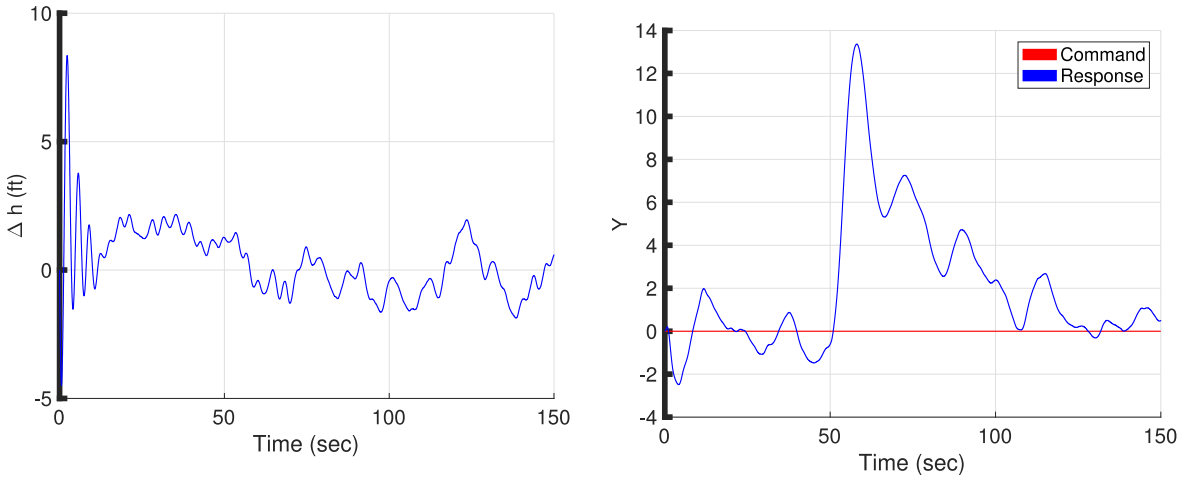


*a*) Altitude error *b*) Horizontal position

Fig. 14. Simulation 3: Altitude error, and horizontal position responses

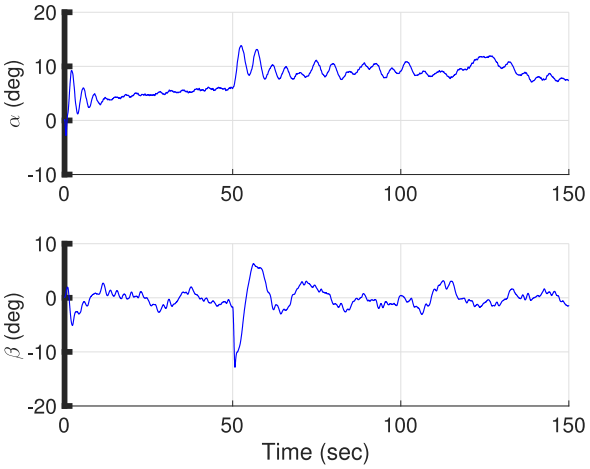


Fig. 15. Simulation 3: Angle of attack and sideslip angle

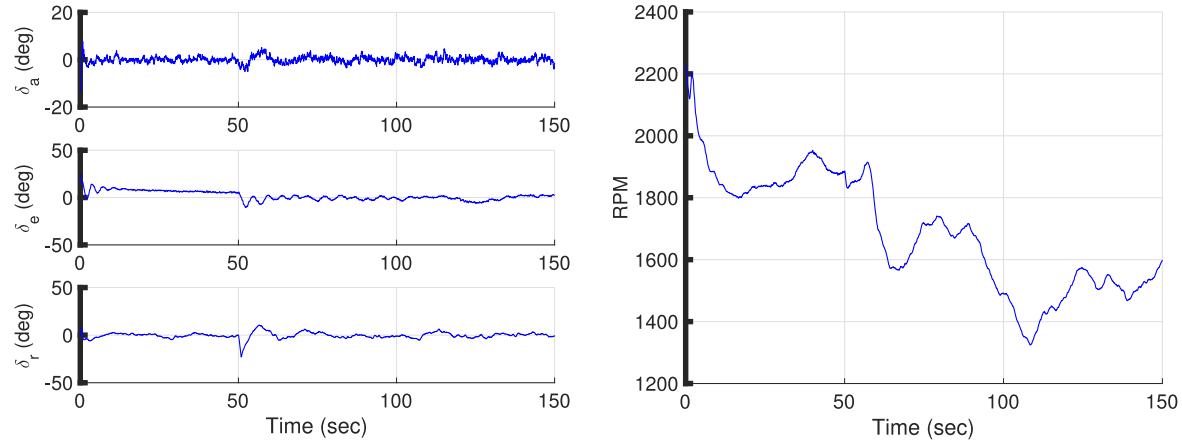


*a*) Aileron, elevator, and rudder positions

*b*) Propeller RPM

Fig. 16. Simulation 2: Altitude error, and horizontal position responses

## Conclusions

This paper presents a flight control system which is based on the SDC dynamic inversion combined with conventional PID control methods. Application of the SDC parameterization for the dynamic inversion removes the need of linearization, and allows to obtain a simple controller structure. The numerical simulations are run to test and validate the effectiveness proposed controller using the Cessna 172 aircraft simulation model. Several simulation scenarios for the airplane stabilization under various atmospheric conditions are tested. The simulation results show the aircraft to maintain the desired altitude, velocity, and follow the given attitude commands.

## References

1. W. Durham, *Aircraft Flight Dynamics and Control*, ser. Aerospace Series. Wiley, 2013. [Online]. Available: https://books.google.com.cy/books?id=dU4fAAAAQBAJ.
2. S. A. Snell, D. F. Enns, and W. L. Garrard, “Nonlinear inversion flight control for a supermaneuverable aircraft,” *Journal of Guidance, Control, and Dynamics*, vol. 15, no. 4, p. 976–984, 1992. Available: https://doi.org/10.2514/3.20932.
3. J. Reiner, G. J. Balas, and W. L. Garrard, “Flight control design using robust dynamic inver- sion and time-scale separation,” *Automatica*, vol. 32, no. 11, pp. 1493–1504, 1996. Available: https://www.sciencedirect.com/science/article/pii/S000510989600101X.
4. G. Wu, X. Meng, and F. Wang, “Improved nonlinear dynamic inversion control for a flexible air-breathing hypersonic vehicle,”Aerospace Science

and Technology, vol. 78, pp. 734–743, 2018. Available: https://www.sciencedirect.com/science/article/pii/S1270963817306168.

5. J. gau Juang, H.-H. Chang, and W.-B. Chang, "Intelligent automatic landing system using time delay neural network controller," *Applied Artificial Intelligence*, vol. 17, no. 7, pp. 563–581, 2003. Available: https://doi.org/10.1080/713827212.
6. S. Singh and R. Padhi, "Automatic path planning and control design for autonomous landing of uavs using dynamic inversion," in *Proc. 2009 American Control Conference*, St. Louis, Missouri, USA, July 2009, p. 2409–2414.
7. R. Lungu and M. Lungu, "Automatic landing control using h-inf control and dynamic inversion," *Proceedings of the Institution of Mechanical Engineers, Part G: Journal of Aerospace Engineering*, vol. 228, no. 14, p. 2612–2626, 2014. Available: https://doi.org/10.1177/0954410014523576.
8. C. P. Mracek and J. R. Cloutier, "Control Designs for the Nonlinear Benchmark Problem via the State-Dependent Riccati Equation Method," *Int. J. Robust Nonlinear. Contr.*, no. 8, pp. 401–433, 1998.
9. J. S. Shamma and J. R. Cloutier, "Existence of SDRE Stabilizing Feedback," *IEEE Trans. Autom. Contr.*, vol. 48, no. 3, pp. 513–517, 2003.
10. T. Cimen, "Systematic and Effective Design of Nonlinear Feedback Controllers via the State-Dependent Riccati Equation (SDRE) method," *Annual Reviews of Control*, vol. 34, pp. 32–51, 2010.
11. M. Korayem and S. Nekoo, "State-Dependent Differential Riccati Equation to Track Control of Time-Varying Systems with State and Control Nonlinearities," *ISA Transactions*, vol. 57, pp. 117–135, 2015.
12. C. P. Mracek, J. R. Cloutier, and C. A. D'Souza, "A New Technique for Nonlinear Estimation," in *Proc. Conf. Contr. Appl.*, Dearborn, MI, September 1996, pp. 338–343.
13. J. Chandrasekhar, A. Ridley, and D. S. Bernstein, "A SDRE-Based Asymptotic Observer for Nonlinear Discrete-Time Systems," in *Proc. Amer. Contr. Conf.*, Portland, OR, June 2005, pp. 3630–3635.
14. A. Berman, P. Zarchan, and B. Lewis, "Comparisons Between the Extended Kalman Filter and the State-Dependent Riccati Estimator," in *AIAA Guid. Nav. Contr. Conf.*, Boston, MA, August 2013.
15. J. Roskam, *Airplane Flight Dynamics and Automatic Flight Controls*. DARcorporation, 1998.